Fluctuations of Coastal Water Temperautres Along Korean and Japanese Coasts in the East Sea*

Yong-Q. KANG and Seong-Won CHOI**
Department of Oceanography, National Fisheries University of Pusan, Pusan.

Based on historic data of monthly means of sea surface temperatures (SST) for 24 years (1921~1944) at 23 Korean and Japanese coastal stations in the East Sea (the Japan Sea), we analyzed spatio-temporal characteristics of coastal SST and SST anomalies. The means of SST at Korean coast are higher than those at Japanese coast of the same latitudes, and the annual range of SST at Korean coast are larger than those at Japanese coast. Empirical orthogonal function analysis shows that almost all (96%) of the SST fluctuations are described by simultaneous seasonal variations.

The fluctuations of SST anomalies are small in the Korea Strait and large at the boundaries between the warm and cold currents in the basin. The fluctuations of SST anomalies along Korean coast are correlated each other. The same is true for SST anomalies along Japanese coast. However, there is only weak correlation between the SST anomalies at Korean coast and those at Japanese coast. Empirical orthogonal function analysis shows that 27% of the coastal SST anomalies in the East Sea are described by simultaneous fluctuations, and 12% of them are described by alternating fluctuations between Korean and Japanese coasts.

Introduction

The East Sea (the Japan Sea) is a semi-enclosed basin, which is connected to the Pacific Ocean through the Korea Strait in the south and the Tsugaru and Soya Straits in the northwest. As shown in Fig. 1, the surface currents in the East Sea consist of the warm currents in the southeastern part and the cold currents in the northwestern part of the basin. The Tsushima Current flows into the basin through the Korea Strait and flows out the basin through the Tsugaru and Soya Straits. The cold currents, such as the Liman and the North Korea Currents, flow southward along Siberian and Korean coasts.

Due to the influences of the ocean currents, the fluctuations of the sea surface temperatures (SST) at the Siberian and Korean coast are expected to be quite different from those at the Japanese coast. The fluctuations of SST in the Tsushima Current region were studied by many authors. Kang and Choi (1985) and Choi and Kang (1987) studied the fluctuations of coastal SST in the Tsushima Current region. The annual march of SST and the fluctuations of SST anomalies off southeastern coast of Korea were studied by Kang and Kang (1987) and Gong and Kang (1986), respectively. However, the relationships between the fluctuations of SST at Korean coast and those at Japanese coast are not well posed yet. In this paper, through analysis of historic

* The present study were supported in part by the Basic Science Research Institute Program, Ministry of Education, 1987. This paper is Contribution No. 203 of the Institute of Marine Sciences, National Fisheries University of Pusan.

**Nuclear Safety Center, Korea Advanced Energy Research Insitute, Daeduk.

data of coastal SST in the East Sea, we study the spatio-temporal characteristics of the fluctuations of SST along the coast of the East Sea. We use the monthly data of only from 1921 to 1944 at 23 coastal stations of Korea and Japan, because the SST data in the northern part of Korea after 1944 are not available. The SST at Siberian coast, which are unavailabe, are not included in this work.

Data and Method

The data set we used is the monthly means of the SST sampled at 5-day interval during 24 years (1921~1944) at 23 coastal stations in the East Sea (Fig. 2). The data set was published by Tokai Regional Fisheries Research Laboratory (Tomosada, 1982).

The seasonal variations of coastal SST are analyzed by the least squares fit of the observed SST of each year at each station to a harmonic function.

$$T(t)=T_0+T_1\cos(\omega t-\phi_1)+T_2\cos(2\omega t-\phi_2) \cdots (1)$$

where t is the time from January 1, T_0 is the annual mean, T_1 and T_2 are the annual and sem-annual amplitudes, respectively, ω is the annual angular frequency, and ϕ_1 and ϕ_2 are the annual and semi-annual phases, respectively. Only annual and semi-annual variations are included in (1), because higher harmonics are negligibly small. Details of the harmonic fitting method can be found in Kang and Jin (1984).

The monthly normals of SST at each station are computed by arithmetic averaging of the SST of the same calender month for 24 years. The SST anomalies at each station are obtained by substracting the monthly normals from the observed monthly SST.

The relative frequency distributions of SST and SST anomalies are computed by counting the numbers of data lying within each interval of 1℃ and 0.5℃, respectively. We computed the regional distribution and the monthly distribution of the root mean squae (rms) amplitudes of SST anomalies. We also computed the cross correlation coefficients between all pairs of SST anomaly series among 23 stations.

The spatio-temporal characteristics of monthly SST and SST anomalies for 24 years (1921~1944) at 23 stations are represented by the empirical orthogonal function (EOF) analysis. In the EOF analysis, a set of time series of temperature, T(x, t), of each length n at m locations is represented by a superposition of EOF modes by

$$T(x,t)=\sum_{i=1}^{m} e_i(x)\, c_i(t) \cdots (2)$$

where $e_i(x)$ is the eigenvector or eigenfunction that describes the spatial distribution of temperatures associated with the i-th mode, and $c_i(t)$ is the time-dependent coefficient that describes the temporal fluctuations of temperature associated with the i-th mode. The eigenvectors and the time-dependent coefficients associated with different modes are orthogonal. That is,

$$\sum_{x=1}^{m} e_i(x)\, e_j(x)=\delta_{ij}$$
$$\sum_{t=2}^{n} c_i(t)\, c_j(t)=n\delta_{ij} \cdots (3)$$

The normalized eigenvectors e can be found by solving an eigenvalue problem

$$Re=\lambda e, \cdots (4)$$

where R is the m by m covariance matrix of the time series at m locations and λ is the eigenvalue. The time-dependent coefficients are proportional to the SST fluctuations associated with each EOF mode. However, due to the orthonormality condition (3), the magnitudes of time-dependent coefficient are not the same as the physical magnitude. More details of the EOF method can be found in Kutzbach (1967).

Seasonal Variation

The seasonal variations of SST for each year during 24 years at 23 coastal stations are fitted to the harmonic function (1).

The 5 harmonic constants (T_0, T_1, T_2, ϕ_1 and ϕ_2) at each station differ from year to year. Table 1 shows the means and the standard deviations of the harmonic constants at 23 stations.

The amplitudes of semi-annual variations are much smaller that those of annual variations. We li-

Table 1. The means and standard deviations of harmonic constants for seasonal varlation of SST for 24 years (1921~1944) at 23 coastal stations in the East Sea.

Station	T_0(℃)	T_1(℃)	ϕ_1(℃)	T_2(℃)	ϕ_2(℃)
A(Cheongjin)	9.6± 0.5	10.6± 0.6	229± 4	1.3± 0.5	111± 17
B(Musudan)	9.0± 0.5	8.8± 0.6	242± 3	1.6± 0.4	116± 13
C(Mayangdo)	10.6± 0.7	10.0± 0.7	230± 4	1.5± 0.4	101± 20
D(Yeodo)	10.9± 0.6	12.1± 0.6	218± 3	0.8± 0.3	131± 41
E(Suweondan)	11.6± 0.8	9.6± 0.8	231± 5	0.7± 0.5	124± 46
F(Jumunjin)	13.6± 0.9	8.6± 0.8	231± 5	0.9± 0.4	125± 61
G(Jukbyon)	14.2± 0.8	6.2± 0.7	237± 6	1.9+ 0.5	131± 36
H(Changgigap)	14.4± 0.8	7.4± 0.7	222± 4	1.1± 0.5	127± 54
I(Pusan)	15.8± 0.5	6.4± 0.5	229± 3	1.1+ 0.4	133± 17
J(Mitsushima)	17.6± 0.5	6.4± 0.6	230± 4	0.8± 0.4	86± 29
K(Okinoshima)	18.9± 0.6	6.4± 0.5	229± 6	0.8± 0.3	94± 44
L(Tsunojima)	17.2± 0.3	7.3± 0.5	227± 3	0.8± 0.3	75± 31
M(Hinomisaki)	18.1± 0.4	7.0± 0.6	232± 3	0.8± 0.3	84± 62
N(Kyogamisaki)	16.8± 0.5	8.0± 0.6	226± 5	0.8± 0.3	102± 74
O(Rokugozaki)	15.8± 0.7	8.7± 0.6	227± 3	0.9± 0.3	83± 31
P(Himesaki)	15.7± 0.8	8.4± 0.8	232± 6	1.1± 0.3	85± 16
Q(Tobishima)	15.1± 0.7	8.6± 0.7	235± 3	1.1± 0.4	74+ 16
R(Nyudozaki)	14.7± 0.6	8.8± 0.7	229± 3	1.1± 0.4	95± 56
S(Shirakamini)	11.8± 0.8	8.3± 1.0	230± 5	1.4± 0.5	111± 18
T(Inahomisaki)	12.5± 0.6	8.5± 0.8	229± 5	1.3± 0.5	107± 27
U(Kamuimisaki)	12.1± 0.4	8.3± 0.7	231± 4	1.2± 0.4	98± 20
V(Yangishiri)	10.7± 0.7	9.2± 0.8	225± 5	1.3+ 0.4	114+ 27
W(Oshidomari)	9.8± 0.6	8.7± 1.0	232± 6	1.2± 0.5	117± 32

mit our discussion to the regional distributions of the annual means, amplitudes, and phases only (Fig. 3).

The mean of SST is high at the Korea Strait (Stations I, J and K) and low at high latitudes. A decrease of the mean SST with distance along Korean coast is rapid whereas that along Japanese coast is mild. The mean of SST at the Station W, which is located at 45°N in Japanese coast, is warmer than those at Stations A and B, which are located at about 42°N in Korean coast. The standard deviations of the means are between 0.5 to 0.8℃.

The annual amplitudes of SST are small at the Korea Strait and large at coastal stations along Korean coast. The annual amplitudes of SST at Stations I, J and K are 6.4℃ and that at Station D is 12.1℃. The standard deviations of annual amplitudes of SST are between 0.6 and 1.0℃.

The annual phases of SST are between 220 to 240°. This means that the SST at coastal stations in the East Sea is maximal between August 20 and September 1. Annual phases at Korean coast show a relatively large difference from station to station (220 to 240°), whereas those at Japanese coast show only a small difference between station to station (225 to 235°).

The frequency distributions of coastal SST differ from station to station. Fig. 4 shows the frequency distributions of SST at Stations D and K. At Station D, where the annual range of SST is large, the SST are distributed in a range of 31℃ (−4 to 27℃). At Station K, where the annual range of SST is small, the SST are distributed in a range of 17℃ (12 to 29℃).

SST Anomalies

The SST anomalies at coastal stations in the East

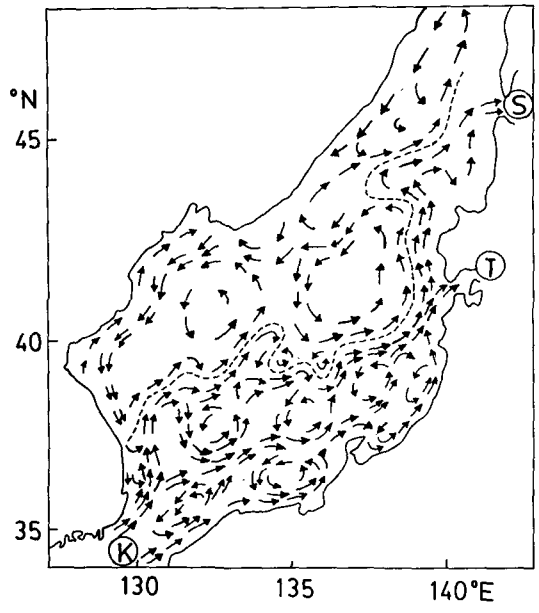

Fig. 1. Surface currents in the East Sea (after Naganuma, 1972). The symbols K, T and S represent the Korea, Tsugaru and Soya Straits, respectively.

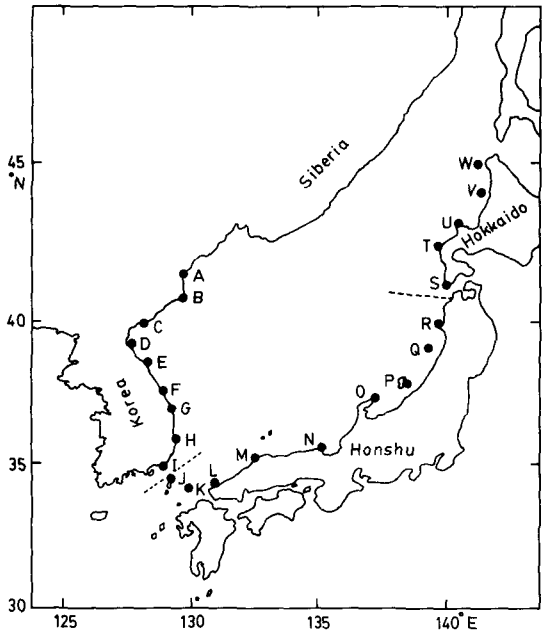

Fig. 2. Coastal Stations in the East Sea.

Sea show irregular fluctuations. The rms amplitudes of monthly SST anomalies for 24 years at 23 coastal stations in the East Sea, shown in Fig. 5, are between 0.8 to 1.5℃. The rms amplitudes of SST anomlies of the Korea Strait (Stations I, J, K and L) are small, and they are less than 1℃. At Stations F and S, which are located near the boundary between the warm and cold currents (see Fig. 1), the rms amplitudes are larger than 1.4℃.

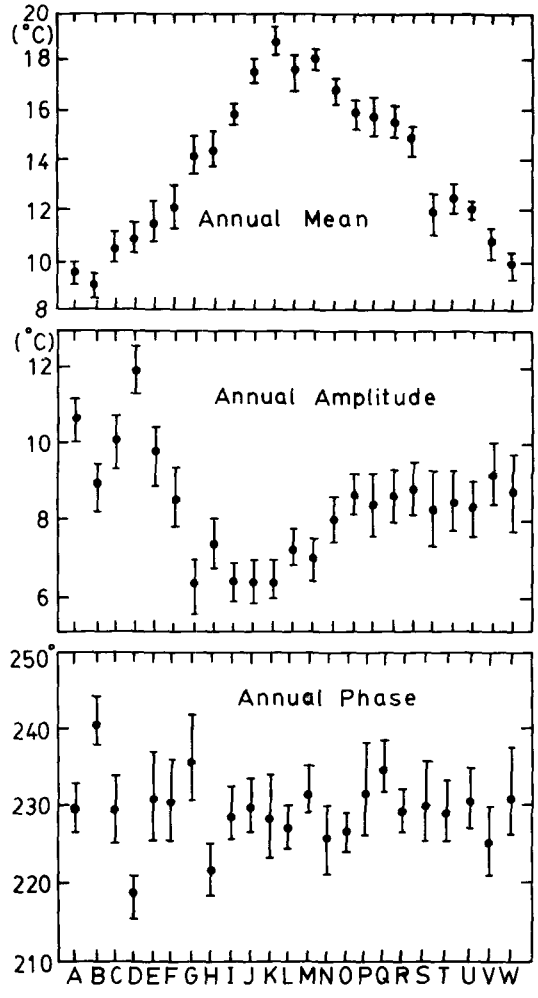

Fig. 3. Regional distribution of the annual means (℃), annual amplitudes (℃) and annual phases (degs) of SST at 23 coastal stations in the East Sea. Vertical bars denote standard deviation over 24 years (1921~1944)

Fig. 6 shows the frequency distributions of SST anomalies of all stations, of Station F, where the rms amplitude is large, and of Station L, where the rms amplitude is small. The frequency distributions of SST anomalies are near Gaussian. At Station F,

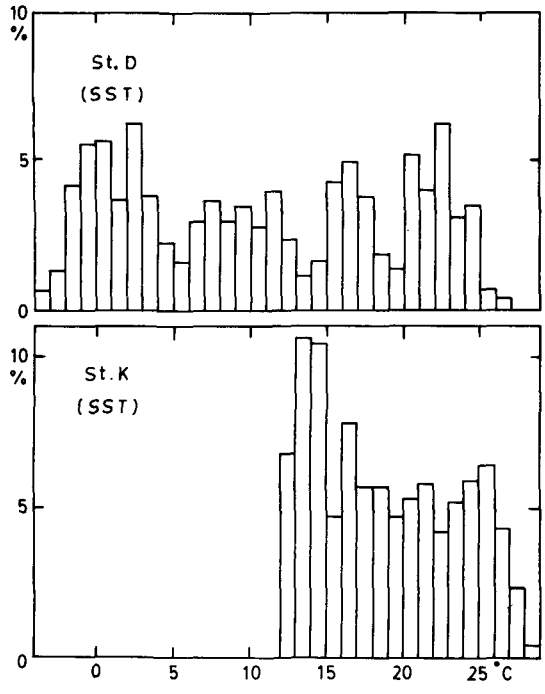

Fig. 4. Frequency distribution of monthly SST at Station D, where annual range is large, and at Station K, where annual range is small.

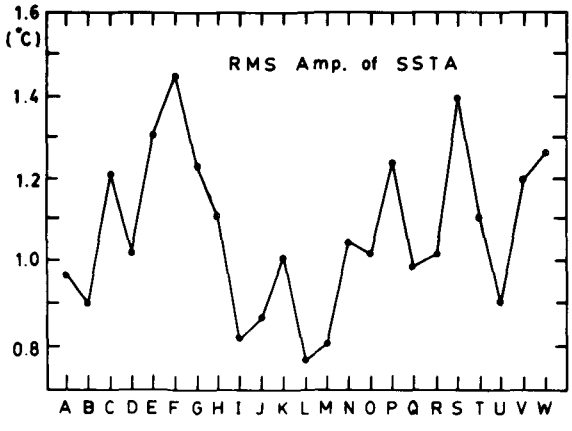

Fig. 5. Regional distribution of rms amplitudes of monthly SST anomalies for 24 years (1921~1944) at 23 coastal stations in the East Sea.

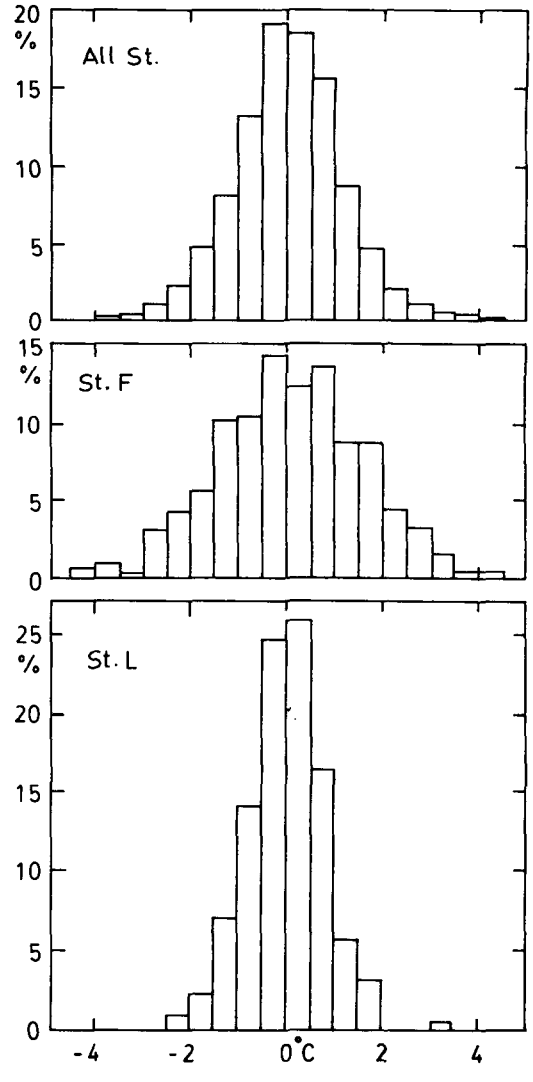

Fig. 6. Relative frequency distributions of SST anomalies for 24 years (1921~1944) at all of 23 stations, at Station F, where rms amplitude is large, and at Station L, where rms amplitude is small.

where the rms amplitude is 1.4℃, the SST anomalies are distributed between −4.5 to 4.5℃. At Station L, where the rms amplitude is only 0.8℃, the SST anomalies are distributed between −2.5 to 2.5℃.

The monthly distributions of the rms amplitudes of SST anomalies at each station are shown in Table 2, and that averaged over 23 stations is shown in Fig. 7. The rms amplitudes are large in summer (July and August) and winter (December and January), and small in spring (March, April and May) and fall (September and October).

Table 2. Monthly distributions of rms amplitudes (℃) of SST anomalies for 24 years (1921~1944) at 23 coastal stations in the East Sea.

Stn.	Jan.	Feb.	Mar.	Apr.	May.	Jun.	Jul.	Aug.	Sep.	Oct.	Nov.	Dec.
A	.93	.83	.67	.77	.70	1.02	1.31	1.35	1.07	0.93	1.15	1.03
B	.70	.82	.75	.70	.73	1.08	1.03	1.35	.95	1.09	1.07	.71
C	.74	.58	.62	.93	1.43	1.51	1.44	1.44	.88	1.35	1.60	1.02
D	1.29	1.00	1.32	1.15	1.20	.90	1.30	.96	.74	.97	1.09	.90
E	1.32	1.38	1.39	1.64	1.62	1.76	1.66	1.57	.92	.66	.91	1.04
F	1.69	1.82	1.74	1.50	1.71	1.67	1.63	1.76	1.09	.70	.87	1.32
G	1.24	1.21	.95	1.33	1.46	1.32	1.76	1.87	1.04	.87	.79	1.02
H	1.20	1.33	1.22	1.03	.88	1.07	1.41	1.48	.98	1.16	1.00	1.33
I	.74	.68	.61	.74	.59	.90	.96	1.42	1.01	.6	.74	.82
J	1.09	1.15	.83	.67	.66	.72	1.03	.89	1.01	.82	.72	1.10
K	1.06	.91	.80	1.19	1.19	1.14	1.43	.84	.99	1.07	1.15	.96
L	.86	.67	.88	.86	.71	.59	1.21	.89	.81	.72	.57	.53
M	.73	.73	.70	.71	.60	.64	1.33	.91	1.10	.81	.78	.57
N	.83	.88	1.08	1.16	1.02	.88	1.37	1.26	1.35	.95	.89	.99
O	1.06	1.11	1.01	1.22	.82	.98	1.38	1.01	.98	.82	1.14	.99
P	1.80	1.47	.95	.84	.77	.78	1.38	1.13	1.06	1.27	1.47	1.96
Q	.98	1.21	1.06	.68	.56	.71	1.15	1.21	1.00	1.10	1.30	1.23
R	1.24	1.27	.87	.77	.94	.89	1.40	1.19	.99	.82	.93	1.22
S	2.06	1.67	1.19	1.14	.91	.96	1.45	1.17	1.27	1.38	1.82	1.80
T	1.27	1.07	.87	1.02	.85	1.06	1.25	1.38	1.04	1.07	1.28	1.56
U	1.03	.87	.69	.54	.95	1.09	1.36	1.12	.80	.87	.75	.95
V	1.23	1.05	.97	.63	1.19	1.08	1.36	1.66	1.20	1.53	1.59	1.33
W	1.67	1.33	.92	.71	1.23	1.15	1.76	1.44	1.16	1.34	1.64	1.57
Avg	1.16	1.09	.96	.95	.98	1.04	1.36	1.27	1.02	1.00	1.10	1.13

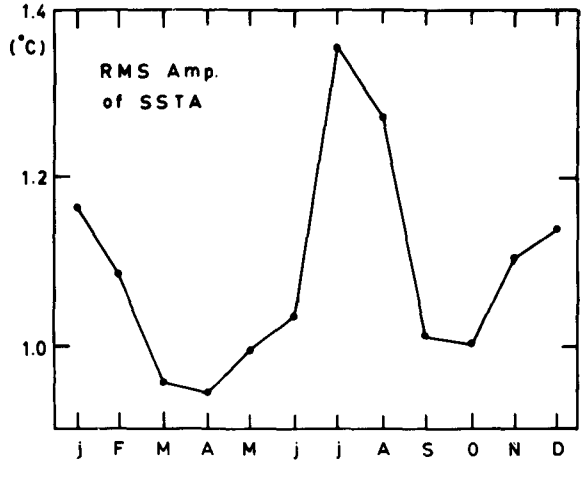

Fig. 7. Monthly distribution of SST anomalies for 24 years (1921~1944) averaged over 23 coastal stations in the East Sea.

The cross-correlation coefficients of SST anomalies between all pairs among 23 stations are shown in Table 3, and the pairs with cross correlations greater than 0.3 are represented by a grey color in Fig. 8. Table 3 and Fig. 8 show that the SST anomalies at stations of Korean coast (Stations A through I) are correlated each other, but they are not correlated with the SST anomalies at Japanese coast (Stations J through W). The same is true for the SST anomalies at Japanese coast. Based on the degree of cress correlations of SST anomalies, the Japanese coast can be grouped into two: the Honshu coast (Stations J to R) and the Hokkaido coast (Stations S to W).

EOF Analysis

1. SST

Table 3. Cross-correlation coefficients (%) of SST anomalies for 24 years (1921~1944) between each pair among 23 coastal stations in the East Sea. The stars (*) indicate auto-correlation coefficients (100%)

Stn.	A	B	C	D	E	F	G	H	I	J	K	L	M	N	O	P	Q	R	S	T	U	V	W
A	*	61	39	41	52	34	18	24	29	17	23	22	20	16	22	-6	27	20	31	21	25	14	23
B	61	*	50	41	58	42	33	23	36	18	18	15	19	11	22	6	29	12	24	19	18	18	19
C	39	50	*	49	43	26	31	38	44	25	13	19	15	14	24	16	24	15	18	16	17	4	11
D	41	41	49	*	51	33	31	28	39	24	10	28	27	21	24	21	42	14	15	8	13	13	9
E	52	58	43	51	*	69	50	34	36	24	17	35	28	25	26	12	28	22	21	12	18	4	13
F	34	42	26	33	69	*	50	31	29	16	11	23	16	21	24	11	23	20	17	4	13	2	-2
G	18	33	31	31	50	50	*	51	43	13	2	12	10	17	13	23	20	12	11	10	12	1	0
H	24	23	38	38	34	31	51	*	57	27	13	17	15	23	30	28	33	29	22	11	14	8	14
I	29	36	44	39	36	29	43	57	*	24	11	18	17	10	28	19	25	21	24	16	9	4	6
J	17	18	25	24	24	16	13	27	24	*	36	31	57	42	29	40	23	19	0	17	17	24	10
K	23	18	13	10	17	11	2	13	11	36	*	36	51	21	18	11	10	11	20	22	14	25	21
L	22	15	19	28	35	23	12	17	18	31	36	*	52	41	41	20	33	27	18	14	19	9	10
M	20	19	15	27	28	16	10	15	17	57	51	52	*	52	36	39	39	22	12	30	24	35	18
N	16	11	14	21	25	21	17	23	10	42	21	41	52	*	52	33	32	16	16	31	30	14	18
O	22	22	24	24	26	24	13	30	28	29	18	41	36	52	*	23	25	29	28	24	22	0	23
P	-6	6	16	21	12	11	23	28	19	40	11	20	39	33	23	*	37	19	-11	27	27	41	12
Q	27	29	24	42	28	23	20	33	25	23	10	33	39	32	25	37	*	34	25	26	27	28	17
R	20	12	15	14	22	20	12	29	21	19	11	27	22	16	29	19	34	*	33	4	23	6	-5
S	31	24	18	15	21	17	11	22	24	0	20	18	12	16	28	11	25	33	*	18	30	0	25
T	21	19	16	8	12	4	10	11	16	17	22	14	30	31	24	27	26	4	18	*	44	37	41
U	25	18	17	13	18	13	12	14	9	17	14	19	24	30	22	27	27	23	30	44	*	38	43
V	14	18	4	13	4	2	1	8	4	24	25	9	35	14	0	41	28	6	0	37	39	*	35
W	23	19	11	9	13	-2	0	14	6	10	21	10	18	18	23	17	17	-5	25	41	43	35	*

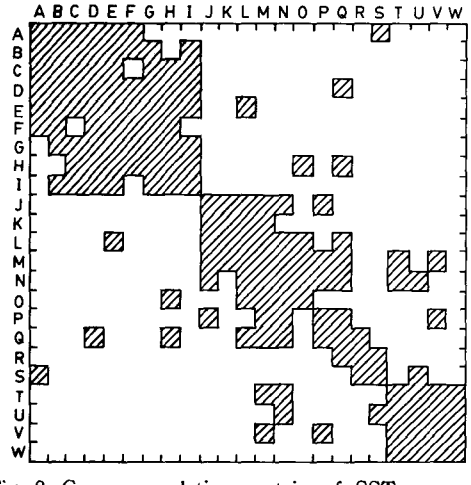

Fig. 8. Cross correlation matrix of SST anomalies among 23 coastal stations in the East Sea. Pairs with a cross correlation coefficient greater than 0.3 are represented by grey color.

The spatio-temporal characteristics of the monthly SST for 24 years (1921~1944) at 23 coastal stations are decomposed into various EOF modes by (2). Fig. 9 shows the eigenfuntions and the associated time-dependent coefficients of the first 3 EOF modes of the monthly SST fluctuations. The fractions of total variance explained by the first 3 EOF modes are 96.4, 0.9 and 0.5%, respectively.

The eigenfunction of the first EOF mode has the same sign at all stations, and the associated time-dependent coefficients vary sinusoidally with an annual cycle. That is, the first EOF mode represents simultaneously-varying seasonal variations.

The time-dependent coefficients of the second EOF mode also vary sinusoidally with an annual cycle, but the sign of the eigenfunction changes from station to station. This indicates that the second EOF mode represents annual fluctuations of which phase differ from station to station. The fluctuations

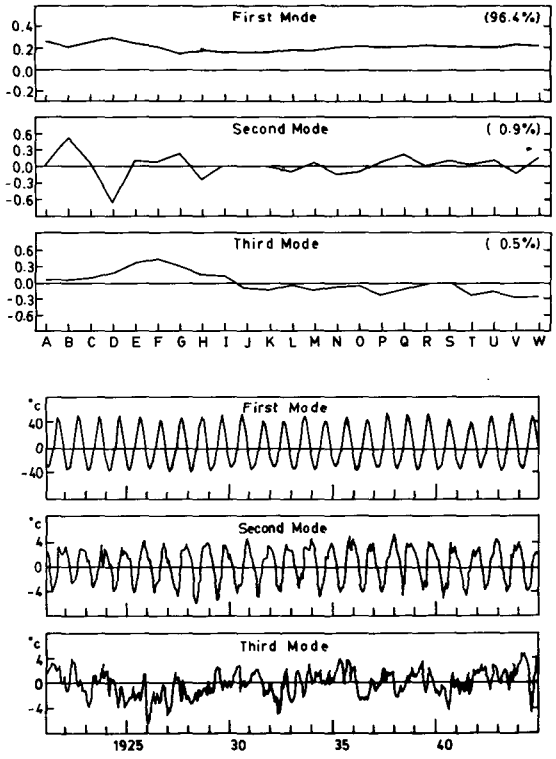

Fig. 9. Eigenfunctions and the associated time-dependent coefficients of the fluctuations of monthly SST for 24 years (1921~1044) at 23 coastal stations in the East Sea. The fractions of the total variance explained by the first 3 EOF modes are 96.4, 0.9 and 0.5%, respectively.

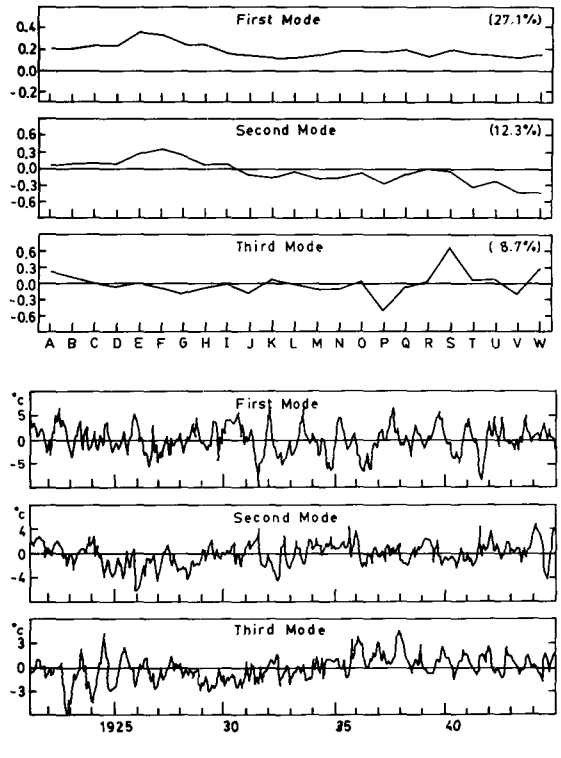

Fig. 10. Eigenfunctions and the associated time-dependent coefficients of the monthly SST anomalies for 24 years (1921~1044) at 23 coastal stations in the East Sea. The fractions of the total variance explained by the first 3 EOF modes are 27.1, 12.3, and 8.7%, respectively.

of SST with an annual period, represented by the first two EOF modes, cover 97.3% of the total variance.

The third EOF mode describes fluctuations with a "seesaw" pattern. That is, the fluctuations along coast (Stations A through I) are opposite to those along Japanese coast (Stations J through W). Although the third EOF mode explains only 0.5% of the variance of SST, this mode represent the seesaw pattern of SST anomalies, as will be shown later.

2. SST Anomalies

Fig. 10 show the eigenfunctions and the associated time-dependent coefficients of the first 3 EOF modes of the SST anomalies for 24 years at 23 coastal stations in the East Sea.

The fractions of total variance explained by the first 3 EOF modes are 27.1, 12.3 and 8.7%, respectively. For the case of SST including the seasonal variation, the first EOF mode alone covers almost all of the variance (96.4%), but for the case of SST anomalies, a superposition of the first 3 EOF modes covers only about one half of the total variance (48.1 %).

The eigenfunction of the first EOF mode of the SST anomalies has the same sign at all stations, and the associated time-dependent coefficients vary irregulary in time. The first EOF mode, which covers 27.1% of the total variance, represents simultaneous fluctuations of SST anomalies at all station.

The second EOF mode, which covers 12.3% of

the total variance, represents seesaw-like fluctuations. In other words, when the fluctuations of SST anomalies associated with the second EOF mode at Korean coast (Stations A to I) are increasing, those in Japanese coast (Stations J to W) are decreasing, and *vice versa*. Note that the eigenfunction and time-dependent. coefficients of the second EOF mode of SST anomalies (Fig. 10) are similar to those of the third EOF mode of SST including seasonal variations (Fig. 9).

The eigenfunction of the third EOF mode, which covers 8.7% of the variance, shows a tendency that the sign at northern part (Stations A through B and R through W, except V) is opposite to that at southern part (Stations C through Q, except K and O).

The third EOF mode crudely represents another seesaw-like fluctuations in which an increase of the SST anomalies in the southern part is accompanied with a decrease in the northern part of the basin, and *vice versa*.

Discussion and Conclusions

In this paper, we showed that the means of SST at Korean coast are lower than those at Japanese coast of the same latitudes, and the annual ranges of SST at Korean coast are larger than those at Japanese coast (Fig. 3). This feature can be understood by considering the fact that, in addition to the radiation budget across the sea surface, the heat advections by ocean currents and the Asian monsoon give substantial influences to the annual variation of SST in the East Sea. According of Kang (1985), the heat advection by warm currents, such as the Kuroshio and the Tsushima Current, increases the means of SST and decreases the annual ranges of SST. On the other hand, the heat advection by cold currents, such as the Liman and the North Korea currents, and also that by the Asian monsoon, decreases the means of SST and increases the annual ranges of SST. The distributions of the means and the annual amplitudes of SST, shown in Fig. 3, is in accordance with the arguments by Kang (1985).

The rms amplitudes of SST anomalies at the Korean Strait are smaller than those at Korean and Japanese coasts (Fig. 5). This means that the interannual fluctuations of SST of the Tsushima Current flowing into the East Sea through the Korea Strait are small but those in the interior of the basin are large. The largest rms amplitudes of SST anomalies are found at Stations F and S, which are located close to the boundaries between the cold and the warm currents in the East Sea (Fig. 1). These facts imply that a large portion of interannual fluctuations of coastal SST anomalies in the East Sea are associated with the shifts in the paths of the ocean currents and with the changes in the strengths of the currents.

The rms amplitudes of SST anomalies in summer and winter are larger than those in spring and fall. Similar features were previously reported for SST anomalies in the Tsushima Current and the Kuroshio regions (Kang and Choi, 1985) and for those in the southwestern East Sea (Gong and Kang, 1986). A similar feature was also reported for the case of monthly air temperature anomalies in Korean peninsula (Kang and Rho, 1985). The rms amplitudes of SST anomalies are maximal in summer, whereas those of air temperature anomalies are maximal in winter.

The EOF analysis showed that almost all of the variance (96.4%) of coastal SST variation are described by simultaneously-varying annual variation. Another 0.9% of SST variation are described by non-simultaneous annual variation. The seesaw-like fluctuations, in which the SST at Korean and Japanese coasts fluctuates alternately, cover 0.5% of the SST fluctuations.

The EOF analysis of SST anomalies shows that about one half of the variance of SST anomalies can be described by a superposition of simultaneous fluctuations (27.1%), alternating fluctuations between Korean and Japanese coasts (12.3%), and another alternating fluctuations between the northern and southern parts of the basin (8.7%). The remaining half of the SST anomalies show irregular fluctuations.

Regional correlations of SST anomalies depend greatly on the pattern of ocean currents. The SST anomlaies at Korean coast, along which the Liman and the North Korean Currents flow southward, are relatively well correlated each other. The SST ano-

malies at Japanese coast, along which the Tsushima Current flows northeastward, are also relatively well correlated each other. But the SST anomalies between Korean and Japanese coasts are not closely correlated.

In this paper, through analysis of historic data of monthly SST for 24 years at 23 coastal stations in the East Sea, we showed that the spatio-temporal characteristics of SST and SST anomalies are closely related with the pattern of the ocean currents in the basin.

References

Choi, S. W. and Kang, Y. Q. 1987. Empirical orthogonal function analysis of coastal water temperatures in the Tsushima Current region. Bull. Kore. Fish. Soc. 20(2), 89~94.

Gong, Y. and Kang, Y. Q. 1986. Sea surface temperature anomalies off the southeastern coast of Korea. Bull. Fish. Res. Dev. Agency 37, 1~9.

Kang, Y. Q. 1985. Influences of the Asian monsoon and the Kuroshio on the sea surface temperatures in the Yellow, the Japan and the East China Seas. J. Oceanol. Soc. Korea 20(2), 1~9.

Kang, Y. Q. and Choi, S. W. 1985. Annual and interannual fluctuations of coastal water temperatures in the Tsushima Current and the Kuroshio regions. Bull. Kor. Fish. Soc. 18(6), 497~505.

Kang, Y. Q. and Jin, M. S. 1984. Seasonal variation of sea surface temperatures in the neighbouring seas of Korea. J. Oceanol. Soc. Korea 19(1), 31~35.

Kang, Y. Q. and Kang, O. G. 1987. Annual variation of water temperatures in the upper 200m off southeast coast of Korea. J. Oceanol. Soc. Korea 22(2), 71~79.

Kang, Y. Q. and Rho, J. S. 1985. Annual and interannual fluctuations of air temperature in Korea during the past 30 years (1954~1983). J. Kor. Meteor. Soc. 21(3), 1~10.

Kutzbach, J. E. 1967. Empirical eigenvectors of sea-level pressure, surface temperature and precipitation complexes over North America. J. Appl. Meteor. 6, 791~802.

Naganuma, K. 1972. The oceanographic conditions in the Japan Sea. In : Handbook of Fisheries Oceanography, Zengyoren Gyokaikyo Center, pp. 32~38 (in Japanese).

Tomosada, A. (Editor). 1982. Monthly Mean Data of Air and Sea Surface Temperatures Measured at the Coast Since 1910 by Assigning to Light Houses and Fisheries Experiment Stations. Datum Collection of Tokai Regional Fisheries Research Laboratory, No. 10, 366 p.

Received October 20, 1988
Accepted December 16, 1988